PAPER

Check for updates

Near-infrared circularly polarized organic room temperature phosphorescence based on a chiral host–guest doping strategy†

Junming Xia,[a] Chenchen Xiong,[a] Songmin Mo,[b] Yongfeng Zhang,[a] Kai Zhang,[a] Gengchen Li,[a] Jianbing Shi, [ID][a] Junge Zhi,[c] Bin Tong, [ID][a] Qinghe Wu, [ID]*[b] Peng Sun,*[d] Zhengxu Cai [ID]*[ae] and Yuping Dong [ID][a]

Achieving high-performance circularly polarized organic room temperature phosphorescence (CPRTP) holds significant academic and industrial importance. Herein, a series of near-infrared, color-tunable, and long-lived CPRTP materials have been successfully constructed by doping achiral luminescent guests into chiral crystallizable hosts. Naphthalimide derivatives are chosen as the guest molecules owing to the large conjugation and good structure tunability. (−)-Di-p-toluoyl-L- and (+)-di-p-toluoyl-D-tartaric acid are selected as the host molecules on account of the outstanding chirality and crystallinity. Through doping naphthalimide into tartaric acid derivatives, the resultant materials show the desirable CPRTP with a luminescence dissymmetry factor equal to 1.14×10^{-2}. The host stabilizes and protects triplet excitons generated from the guest and induces the chirality of phosphorescence. Impressively, the doping material is emissive in the near-infrared region of 720 nm, which has hardly been achieved before. By modifying the chemical structure of the guest, the phosphorescent color of doping materials can be well-modulated from green to yellow and red. Moreover, the doping material displays a lifetime of up to 2.14 s. It is highly anticipated that this work will provide a new design strategy for high-performance CPRTP materials.

1. Introduction

Taking the advantage of the large Stokes shift, low cell toxicity, and relatively long excited-state lifetime, organic room temperature phosphorescence (RTP) materials have shown great application potential in bioimaging, optoelectronic devices, and encryption storage fields.[1–9] As a further development in this field, circularly polarized organic room temperature phosphorescence (CPRTP) has received widespread attention and

[a] Beijing Key Laboratory of Construction Tailorable Advanced Functional Materials and Green Applications, School of Materials Science and Engineering, Beijing Institute of Technology, Beijing 100081, China. E-mail: caizx@bit.edu.cn

[b] Department of Chemistry and Key (Guangdong-Hong Kong Joint) Laboratory for Preparation and Application of Ordered Structural Materials of Guangdong, Shantou University, Shantou, Guangdong 515063, China. E-mail: wuqh@stu.edu.cn

[c] Key Laboratory of Cluster Science of Ministry of Education, School of Chemistry and Chemical Engineering, Beijing Institute of Technology, Beijing 100081, China

[d] Advanced Research Institute of Multidisciplinary Science, Beijing Institute of Technology, Beijing 100081, China. E-mail: sunpeng@bit.edu.cn

[e] Tangshan Research Institute, Beijing Institute of Technology, Beijing 100081, China

† Electronic supplementary information (ESI) available. CCDC 2353069 and 2353070. For ESI and crystallographic data in CIF or other electronic format see DOI: https://doi.org/10.1039/d4tc01828a

Zhengxu Cai

Prof. Zhengxu Cai received his BS degree from Wuhan University in 2009, and obtained PhD from Institute of Chemistry, Chinese Academic of Science in 2014 under the supervision of Prof. Deqing Zhang. After a post-doctoral study at Prof. Luping Yu's group in University of Chicago, he joined School of Material Science and Engineering at Beijing Institute of Technology (BIT) in 2017. He is now a professor in BIT. His research focuses on host–guest doping systems towards organic room-temperature phosphorescence (RTP). A series of high performance RTP materials were developed for anti-counterfeiting and high-resolution bioimaging.

9578 | *J. Mater. Chem. C,* 2024, **12**, 9578–9585

This journal is © The Royal Society of Chemistry 2024

undergone in-depth exploration in recent years.[10–13] The CPRTP material can emit left- or right-handed RTP with mirror symmetric characteristics.[14–16] This unique optical property enables the CPRTP material for application in three-dimensional displays, anti-counterfeiting, and organic light-emitting diodes.[17,18] In the past few years, rational design strategies, including covalent and non-covalent ones, have been developed to realize CPRTP.[19–21] The covalent strategy involves incorporating chiral centers with RTP structures through chemical modification or polymerization, which holds the advantages of structural stability and property tunability.[22–24] Meanwhile, CPRTP achieved *via* non-covalent interactions among chiral molecules and RTP materials, such as crystal engineering and host–guest doping methods, offers the advantages of simple preparation and production scalability.[25–27] Despite tremendous progress being made, constructing high-performance CPRTP materials remains a formidable task. CPRTP materials still suffer from many limitations, such as short wavelength, which severely hinder the further development and application of CPRTP materials.

Organic near-infrared luminescent materials are known as organic molecules or polymeric materials with emission wavelengths ranging from 700 to 2500 nm.[28–31] RTP materials exhibit a large Stokes shift, which endows them with inherent advantages in the construction of near-infrared luminescent materials.[32–35] However, the relatively high energy level of the excited state, inefficient intersystem crossing process (ISC) and the instability of triplet excitons always result in serious challenges in developing RTP materials with near-infrared emission.[36,37] Through rational molecular design principle such as enlarging the conjugation, the energy levels of the

triplet excited state have been significantly lowered.[38,39] By introducing heavy atoms, heteroatoms, and carbonyl groups, the ISC process can be greatly enhanced on account of the spin–orbit coupling (SOC) effect.[40] Meanwhile, through host–guest doping, crystallization, and supramolecular self-assembly, the generated triplet excitons with low excited energy can be stabilized from non-radiative relaxation and protected from reactants effectively.[41,42] To date, research on organic near-infrared RTP materials mainly focuses on extending the emission wavelengths, increasing exciton lifetimes, and improving luminescence efficiency.[43–45] Explorations of organic near-infrared RTP materials with circularly polarized emission have rarely been well investigated. The circularly polarized luminescence characteristic contributes to extending the applications of near-infrared RTP materials to information security, biological imaging, and three-dimensional displays.[46–52] Therefore, the development of near-infrared CPRTP materials is in urgent and substantial demand.

In this work, near-infrared CPRTP materials were constructed through doping the achiral guest molecules with near-infrared phosphorescence emission into the chiral host molecules with excellent crystallinity. To realize CPRTP with long emission wavelength, the guest molecule should not only have strong abilities of absorbing photons and generating triplet excitons but also possess large conjugation structures.[53–57] As shown in Scheme 1a, six naphthalimide derivatives, denoted as **NI-I**, **NI-II**, **NDI**, **NDI-Br**, **NTI**, and **NTI-Br**, respectively, are designed, synthesized and chosen as the achiral guest molecules.[58] The large conjugation between benzene rings, benzene rings and carbonyl groups, and carbonyl groups and nitrogen
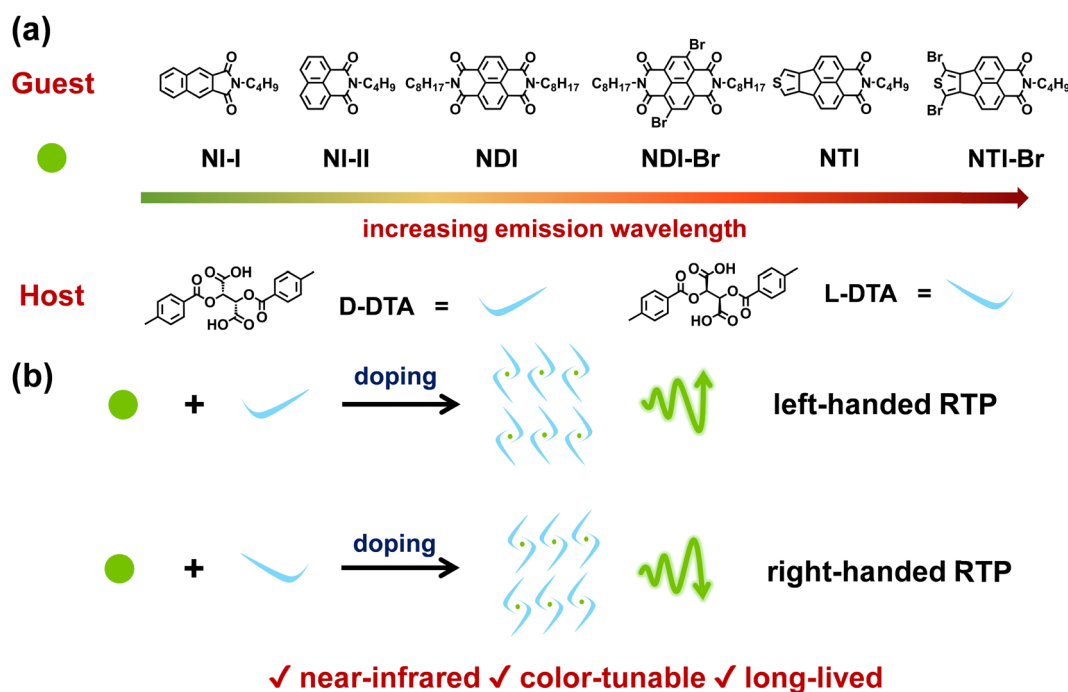
Scheme 1 (a) The chemical structures of the naphthalimide derivative guest molecules and the D- and L-DTA host molecules. (b) The schematic diagrams of the near-infrared CPRTP achieved through a host–guest doping strategy.

This journal is © The Royal Society of Chemistry 2024

J. Mater. Chem. C, 2024, **12**, 9578–9585 | **9579**

atoms, endows naphthalimide derivatives with a good photon absorbing ability and exciton generating ability, and a low energy gap.[43,59] Meanwhile, bromine heavy atoms, carbonyl groups, and heteroatoms like nitrogen and sulfur enhance the ISC process on account of the spin-orbital coupling and heavy atom effect.[60,61] (−)-Di-p-toluoyl-L- and (+)-di-p-toluoyl-D-tartaric acid (L-DTA and D-DTA) are a pair of enantiomers and are selected as the chiral host molecules to realize near-infrared CPRTP. Both L- and D-DTA possess excellent crystallinity, which contributes to stabilizing and protecting triplet excitons. More importantly, L- and D-DTA can potentially induce the chirality of phosphorescence because of their enantiomer nature (Scheme 1b). After doping naphthalimide derivatives into DTA, the resultant materials are endowed with the desirable RTP with a luminescence dissymmetry factor (g_{lum}) of 1.14×10^{-2}. More importantly, the emission wavelength of the doping material reaches as long as a near-infrared region of 720 nm, which is difficult to be achieved in previous studies. The emission color can be well-modulated from green to yellow and red by changing the guest molecule. In addition, the lifetime of host–guest doping materials

can extend up to 2.14 s at maximum. Therefore, a series of CPRTP materials with near-infrared emission, color-tunability, and long lifetime are successfully constructed via doping achiral naphthalimide derivative guest molecules into chiral DTA host molecules.

2. Results and discussion

The chemical structures of the synthesized naphthalimide derivatives are directly confirmed using the ^{1}H-NMR, ^{13}C-NMR, and mass spectra (Fig. S1–S18, ESI†). To investigate their photophysical properties, the UV-Vis absorption and photoluminescence (PL) spectra were recorded. As shown in Fig. 1a, the naphthalimide derivatives exhibit strong absorptions below 300 nm, which are attributed to the B-band absorption of the benzene ring. They also have significant absorptions above 300 nm, and the absorption peaks of **NI-I**, **NI-II**, **NDI**, **NDI-Br**, **NTI**, and **NTI-Br** are located at 292, 331, 378, 361, 379, and 428 nm, respectively,
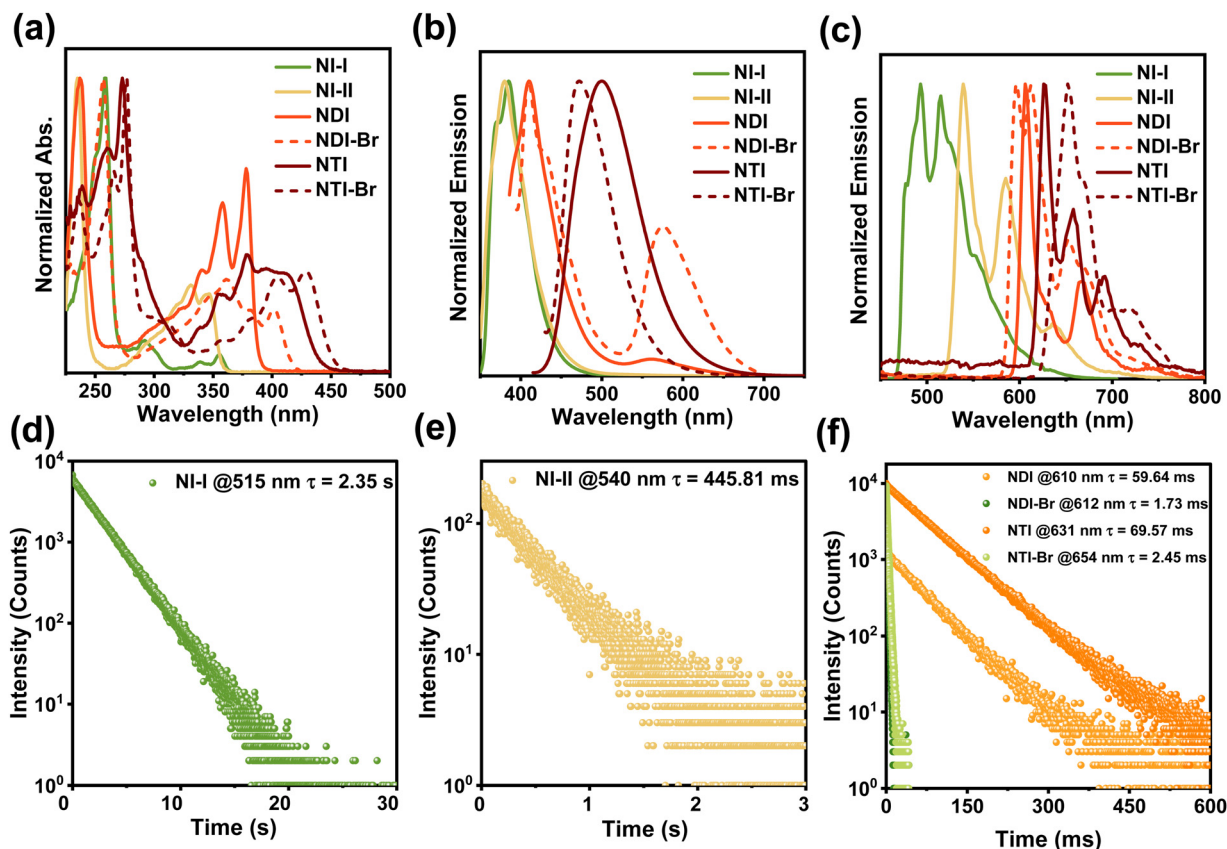
Fig. 1 (a) The UV-Vis spectra of **NI-I**, **NI-II**, **NDI**, **NDI-Br**, **NTI**, and **NTI-Br**, respectively (the concentration is 1×10^{-5} M in tetrahydrofuran). (b) The fluorescence spectra of **NI-I**, **NI-II**, **NDI**, **NDI-Br**, **NTI**, and **NTI-Br**, respectively (the concentration is 1×10^{-5} M in tetrahydrofuran, the **NI-I** and **NI-II** are excited under 340 nm irradiation, the **NDI** and **NDI-Br** are excited under 360 nm irradiation, and **NTI** and **NTI-Br** are excited under 405 nm irradiation). (c) The phosphorescence spectra of **NI-I**, **NI-II**, **NDI**, **NDI-Br**, **NTI**, and **NTI-Br**, respectively (the concentration is 1×10^{-5} M in 2-methyltetrahydrofuran, the **NI-I** and **NI-II** are excited under 340 nm irradiation, the **NDI** and **NDI-Br** are excited under 360 nm irradiation, **NTI** and **NTI-Br** are excited under 405 nm irradiation, and the delayed time is 50 μs). (d) The lifetime profile of **NI-I** (the concentration is 1×10^{-5} M in 2-methyltetrahydrofuran and the excitation wavelength is 340 nm). (e) The lifetime profile of **NI-II** (the concentration is 1×10^{-5} M in 2-methyltetrahydrofuran and the excitation wavelength is 340 nm). (f) The lifetime profiles of **NDI**, **NDI-Br**, **NTI**, and **NTI-Br**, respectively (the concentration is 1×10^{-5} M in 2-methyltetrahydrofuran, the **NDI** and **NDI-Br** are excited under 360 nm irradiation, and **NTI** and **NTI-Br** are excited under 405 nm irradiation).

9580 | J. Mater. Chem. C, 2024, **12**, 9578–9585

This journal is © The Royal Society of Chemistry 2024

corresponding to the absorption of the naphthalimide structure. As shown in Fig. 1b, naphthalimide derivatives display significant fluorescence emission, and the emission peaks of **NI-I**, **NI-II**, **NDI**, **NDI-Br**, **NTI**, and **NTI-Br** appear at 385, 380, 410, 410 and 576, 500, and 472 nm, respectively, indicating that naphthalimide derivatives have strong exciton generation abilities. Their fluorescent color can be well-tuned from blue to cyan and red by extending the conjugation and incorporating donor–acceptor interaction, and the emission wavelengths gradually redshift accordingly. A similar redshift is also observed in the delayed PL spectra of naphthalimide derivatives at 77 K. As shown in Fig. 1c, the strongest cryogenic phosphorescence emission peaks of **NI-I**, **NI-II**, **NDI**, **NDI-Br**, **NTI**, and **NTI-Br** increase from 493 to 539, 606, 596, 626, and 652 nm, respectively. Notably, owing to the multi-peaked emission characteristic of the naphthalimide structure, the emission peaks of **NTI-Br** can extend to the near-infrared region of 720 nm, making it promising as a guest molecule to realize near-infrared CPRTP.

To further study the photophysical properties of naphthalimide derivatives, the lifetime of their cryogenic phosphorescence was evaluated. As shown in Fig. 1d–f, the phosphorescence lifetimes of **NI-I**, **NI-II**, **NDI**, **NDI-Br**, **NTI**, and **NTI-Br** at 77 K are 2.35 s, 445.81, 59.64, 1.73, 69.57, and 2.45 ms, respectively. Compared with naphthalimide derivatives without bromine atoms, **NDI-Br** and **NTI-Br** have a relatively short phosphorescence lifetime. On the one hand, the introduction of bromine atoms contributes to enhancing the ISC process owing to the heavy atom effect. On the other hand, the incorporation of bromine atoms accelerates phosphorescence radiation decay rates, which results in a sharp decrease in the phosphorescence lifetime. Therefore, all of these results confirm that the naphthalimide derivative guest molecule with the ability to emit near-infrared phosphorescence is successfully constructed.

Density functional theory and SOC constant calculations of the naphthalimide derivatives were conducted to theoretically investigate their emission properties. As shown in Fig. 2, the electron clouds of the highest occupied and the lowest unoccupied molecular orbital are well-distributed over the entire backbone of the naphthalimide derivative, indicating a strong electron delocalization of the guest molecules. The calculated energy of the triplet excited state of **NI-II** and **NDI** decreases from 2.58 to 2.27 eV, and that of **NI-II** and **NTI** decreases from 2.58 to 2.21 eV, which result from the enlarging of conjugation
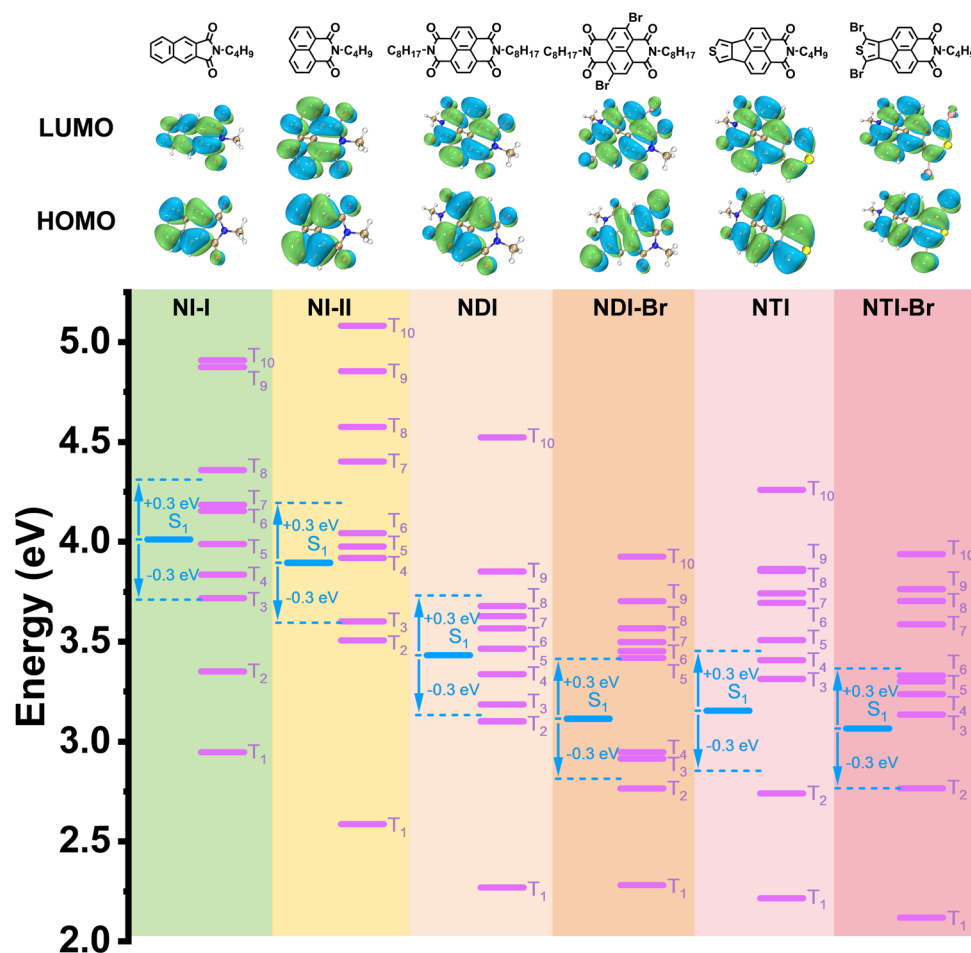

Fig. 2 The density functional theory and SOC constant calculation results of **NI-I**, **NI-II**, **NDI**, **NDI-Br**, **NTI**, and **NTI-Br**, respectively (performed in Gaussian 09 and OCRA programs using the PBE0/def2-TZVP base group).

This journal is © The Royal Society of Chemistry 2024

J. Mater. Chem. C, 2024, **12**, 9578–9585 | **9581**

by introducing the carbonyl groups, double bonds, and hetero-atoms. Molecules with a narrow energy gap between the lowest triplet excited state (T_1) and the ground state (S_0) always show phosphorescence emission with long-wavelength, and these theoretical calculation results are consistent with the observed phenomenon that both **NDI** and **NTI** have longer emission wavelength than **NI-II**. The SOC constant between the singlet and triplet states can be applied to access the ability of naphthalimide derivatives to take place in ISC and emit phosphorescence. The SOC constant between S_1 and T_n of naphthalimide derivatives is substantially improved compared with that of that without bromine atoms, which is attributed to the heavy atom effect. For example, the SOC constant of S_1 to T_5 increases significantly from 13.15 cm^{-1} of **NDI** to 274.61 cm^{-1} of **NDI-Br**, and the SOC constant of S_1 to T_4 of **NTI-Br** (11.30 cm^{-1}) is much higher than that of **NTI** (4.33 cm^{-1}) (Table S1, ESI†). These computational results theoretically demonstrate that naphthalimide derivatives with a large conjugated structure and heavy atoms have the ability to emit near-infrared phosphorescence.

We wonder whether DTA can be employed as the host molecules to realize near-infrared RTP. To answer this question, the steady and delayed PL spectra of DTA and naphthalimide derivatives@DTA doping materials were collected. The host–guest doping materials were prepared though solvent evaporation, and the detailed procedure is discussed in the ESI.† The chemical structure and high purity of commercially available DTA are confirmed using H-NMR, C-NMR, mass spectra, and single-crystal data (Fig. S19–S25 and Tables S2 and S3, ESI†). L- and D-DTA only have strong absorptions below 300 nm, which originate from the B-band of the phenyl ring (Fig. S26, ESI†). As shown in Fig. 3a, all doping materials display strong RTP, which demonstrates that the DTA can stabilize and protect the triplet excitons from non-radiative relaxation. The strongest phosphorescence peaks of **NI-I**, **NI-II**, **NDI**, **NDI-Br**, **NTI**, and **NTI-Br**@DTA are located at 499 to 540, 614, 623, 632, and 662 nm, respectively. More importantly, one of the emission peaks of **NTI-Br**@DTA is located at the near-infrared region of 720 nm, confirming that near-infrared RTP can be achieved through a doping strategy. Moreover, as shown in Table 1, the prepared doping material features decent quantum yields, and the quantum yields of **NI-I**, **NI-II**, **NDI**, **NDI-Br**, **NTI**, and **NTI-Br**@DTA's RTP are 7.58, 1.71, 1.27, 4.84, 0.61, and 1.39%,
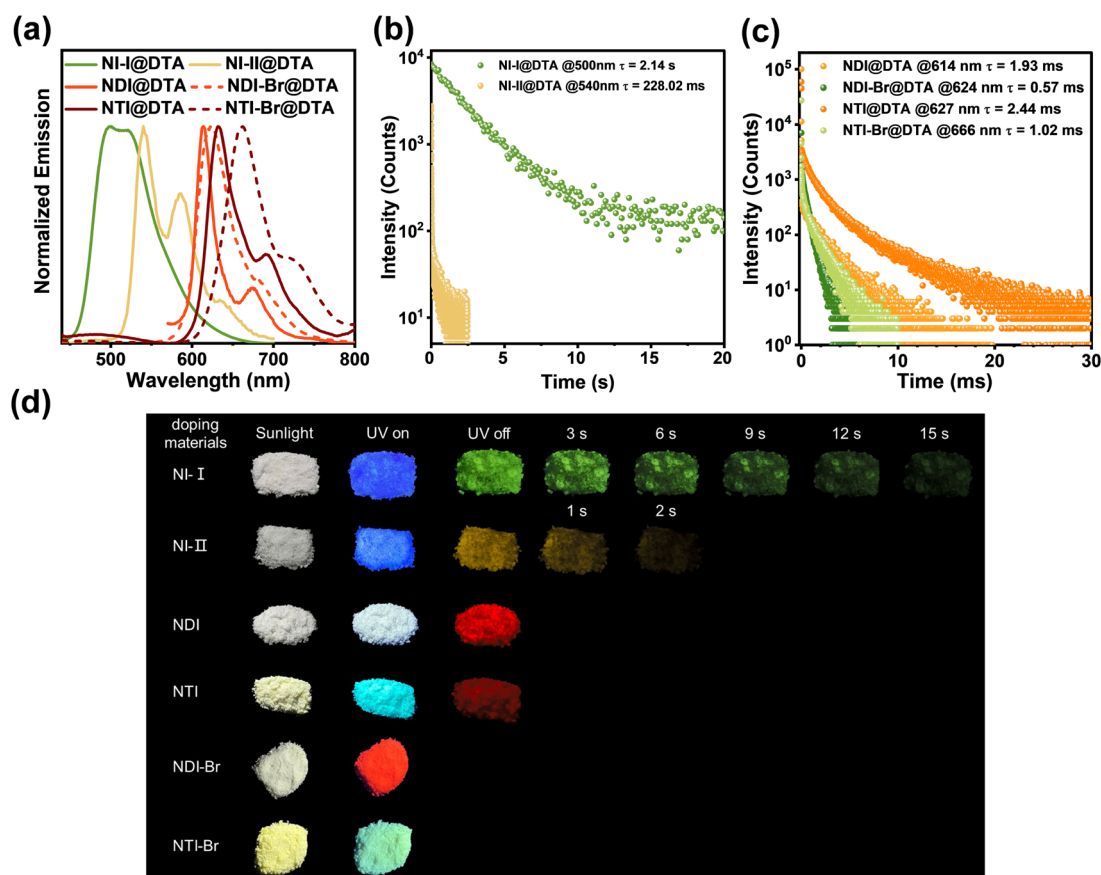

Fig. 3 (a) The phosphorescence spectra of **NI-I**, **NI-II**, **NDI**, **NDI-Br**, **NTI**, and **NTI-Br**@DTA, respectively (the doped molar ratios are 1 : 500 (**NI-I**@DTA), 1 : 1000 (**NI-II**@DTA), 1 : 2500 (**NDI**, **NDI-Br**, **NTI**, and **NTI-Br**@DTA), the **NI-I** and **NI-II**@DTA are excited under 340 nm irradiation, the **NDI** and **NDI-Br**@DTA are excited under 360 nm irradiation, **NTI** and **NTI-Br**@DTA are excited under 405 nm irradiation, and the delayed time is 50 μs). (b) The lifetime profiles of **NI-I** and **NI-II**@DTA (the excitation wavelength is 340 nm). (c) The lifetime profiles of **NDI**, **NDI-Br**, **NTI**, and **NTI-Br**@DTA, respectively (**NDI** and **NDI-Br**@DTA are excited under 360 nm irradiation and **NTI** and **NTI-Br**@DTA are excited under 405 nm irradiation). (d) Digital pictures of **NI-I**, **NI-II**, **NDI**, **NDI-Br**, **NTI**, and **NTI-Br**@DTA, respectively, under 365 nm UV light on and off.

9582 | *J. Mater. Chem. C*, 2024, **12**, 9578–9585

This journal is © The Royal Society of Chemistry 2024

Table 1 Photophysical data of doped materials

Guest@DTA	Fluorescence				Phosphorescence			
	λ_{em} (nm)	τ (ns)	Φ (%)	g_{max}^F	λ_{em} (nm)	τ (ms)	Φ (%)	g_{max}^P
NI-I	383	7.30	14.78	0.0114	499, 521	2140.98	7.58	0.0106
NI-II	398	6.26	0.93	0.0114	540, 586	228.02	1.71	0.0084
NDI	413	5.51	0.42	—	614, 675	1.93	1.27	—
NDI-Br	453	9.05	0.59	—	623, 684	0.57	4.84	0.0166
NTI	487	3.04	2.35	—	632, 690	2.44	0.61	—
NTI-Br	481	2.48	0.61	0.0126	662, 720	1.02	1.39	0.0114

The g_{max}^F represents the fluorescence maximum asymmetry factor value. The g_{max}^P represents the phosphorescence maximum asymmetry factor value. The excitation wavelength of **NI-I** and **NI-II** is 340 nm. The excitation wavelength of **NDI** and **NDI-Br** is 360 nm. The excitation wavelength of **NTI** and **NTI-Br** is 405 nm. The delayed time is 50 µs.

respectively. By virtue of the heavy atom effect, the naphthalimide derivative with bromine atoms is endowed with a higher quantum yield than that of the naphthalimide derivative with bromine atoms. The doping ratio plays a significant role in the RTP intensity. As shown in Fig. S28 (ESI†), as the guest content decreases, the RTP intensity of the doped material initially increases and then decreases. Each doping material has an optimal doping ratio, and subsequent research is based on this optimal doping ratio. When the guest molecule content is high, the undesired triplet–triplet annihilation may result in weak RTP. Meanwhile, when the guest molecule content is low, the reduced number of luminescence centers will also lead to low RTP intensity.

The mechanism of photophysical properties is further investigated. As shown in Table 1 and Fig. 1c and 3a, the emission peaks of doping materials are consistent with the cryogenic delayed emission of naphthalimide derivatives, and the cryogenic phosphorescence curves of guest molecules closely resemble the RTP curves of the doping materials. These phenomena demonstrate that the guest molecules can well-disperse within the host molecules, much like they do in solution, and the RTP originates from the guest instead of host molecules. Meanwhile, the negligible shift in the emission peak

also indicates that the DTA host molecule has no significant effect on the energy levels of the naphthalimide derivative. Under the same radiation, L- and D-DTA are non-emissive in either steady or delayed PL spectra due to the small-conjugation. The fluorescence and phosphorescence spectra of naphthalimide derivative@L-DTA and naphthalimide derivative@D-DTA are consistent in terms of intensity, shape, and peak positions (Fig. S29 and S30, ESI†). As shown in Fig. 3b and c, the phosphorescence lifetimes of **NI-I**, **NI-II**, **NDI**, **NDI-Br**, **NTI**, and **NTI-Br**@DTA at room temperature are 2.14 s, 228.02, 1.93, 0.57, 2.44, and 1.02 ms, respectively. The phosphorescence lifetimes of doping materials exhibit a similar trend to that of guest molecules, and the lifetime decreases sharply with the conjugation enlarging and the introduction of bromine atoms. The lifetime of **NI-I**@DTA RTP is slightly shorter than that of **NI-I**. However, the lifetime of other doping material RTP decreases sharply compared with that of guest molecule cryogenic phosphorescence. Reasons behind this phenomenon could be the molecular size difference. **NI-I** has the smallest molecular size, which makes **NI-I** easily embed into the crystalline lattice of the host. The strong interaction between the host and guest stabilized triplet excitons.
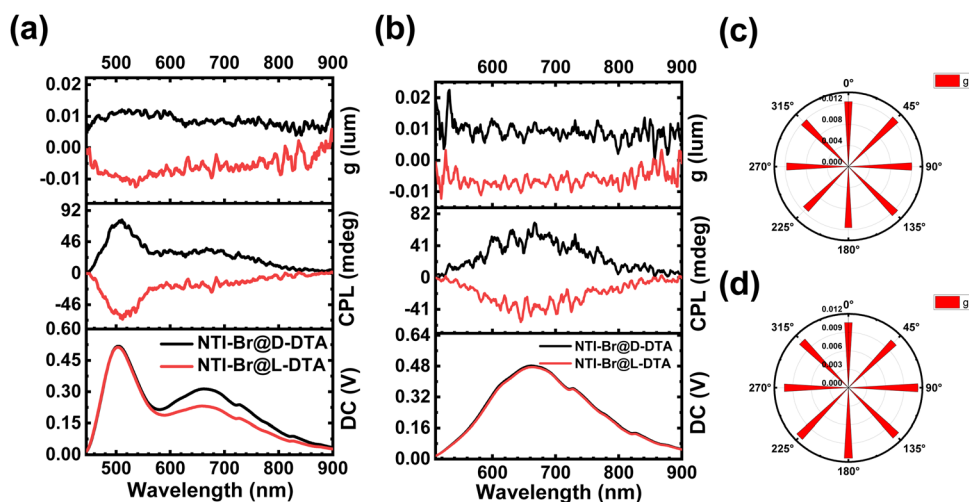

Fig. 4 (a) The circularly polarized luminescence spectra of **NTI-Br**@DTA excited under 405 nm irradiation. (b) The circularly polarized luminescence spectra of **NTI-Br**@DTA excited under 405 nm irradiation with a 570 nm bandpass filter. The g_{lum} of **NTI-Br**@DTA circularly polarized luminescence spectra (c) without and (d) with a 570 nm bandpass filter at different angles.

This journal is © The Royal Society of Chemistry 2024

J. Mater. Chem. C, 2024, **12**, 9578–9585 | **9583**

Owing to the long excited-state lifetimes of doped materials, their RTP performance can be visualized through optical images. As shown in Fig. 3d, the **NI-I**@DTA exhibits a green afterglow of approximately 15 s, while **NI-II**@DTA shows a yellow afterglow of about 2 s, and **NDI**@DTA and **NTI**@DTA display a shorter red afterglow. The afterglow of **NDI-Br**@DTA and **NTI-Br**@DTA are not observable to the naked eye due to a significantly shortened lifetime caused by the heavy atom effect. This phenomenon also indicates that the RTP color can be well-modulated by changing the guest molecules.

To figure out whether the L- and D-DTA host molecules can induce chirality of RTP, the circular dichroism spectra of host molecules and doping materials were obtained. The circular dichroism spectra of L- and D-DTA in both solid and solution states show significant symmetric Cotton effects within their absorption ranges, indicating the enantiomeric structure of the host and good ground-state optical activity (Fig. S31, ESI†). Notably, as shown in Fig. 4a–d, **NTI-Br**@DTA is endowed with the desirable circularly polarized emission, and the g_{lum} of its fluorescence and phosphorescence emission peak is measured to be 1.26×10^{-2} at 511 nm and 1.14×10^{-2} at 667 nm. Owing to the excellent chirality of DTA, the doping materials are endowed with decent g_{lum}. Similar to **NTI-Br**@DTA, **NI-I**, **NI-II**, and **NDI-Br**@DTA also exhibit CPRTP (Fig. S32–S38, ESI†). However, the observation of **NDI** and **NTI**@DTA was unsuccessful due to the relatively low phosphorescence intensities. Therefore, all of these results demonstrate that L- and D-DTA act as the host molecules to induce the chirality of emission.

3. Conclusion

In summary, we have successfully developed a series of novel CPRTP materials with near-infrared emission, color tunability, and long lifetime through doping achiral naphthalimide derivative guest molecules into chiral DTA host molecules. Through enlarging conjugation and introducing bromine heavy atoms, the naphthalimide derivative with cryogenic phosphorescence emission extending to the near-infrared region of 720 nm is constructed. The theoretical calculation results also support our molecular design strategies. By doping naphthalimide derivatives into DTA, the resultant doping materials display strong RTP, the emission color can be well-modulated from green to yellow, red, and near-infrared, and the lifetime can reach as high as 2.14 s. Notably, the chiral host molecule induces the chirality of RTP, and the doping materials exibit the desirable CPRTP with a g_{lum} equal to 1.14×10^{-2}. It is highly anticipated that this line of research will open a new avenue for designing RTP materials with good photo performance and multiple functionalities.

Author contributions

Junming Xia: experimental execution, testing, data analysis, and manuscript preparation; Chenchen Xiong: experimental execution and testing; Songmin Mo: molecule synthesis; Yongfeng Zhang, Kai Zhang, Gengchen Li, Jianbing Shi, Junge Zhi, and Bin Tong: data analysis; Qinghe Wu: supervision, molecular design, and data analysis; Peng Sun: supervision, data analysis, and manuscript preparation; Zhengxu Cai: supervision, research design, data analysis, and manuscript preparation; Yuping Dong: supervision, conceptualization, data analysis, and manuscript preparation.

Conflicts of interest

The authors declare no conflict of interest.

Acknowledgements

References

1 X. Ma, J. Wang and H. Tian, *Acc. Chem. Res.*, 2019, **52**, 738.
2 Z. Yang, C. Xu, W. Li, Z. Mao, X. Ge, Q. Huang, H. Deng, J. Zhao, F. L. Gu, Y. Zhang and Z. Chi, *Angew. Chem., Int. Ed.*, 2020, **59**, 17451.
3 H. Peng, G. Xie, Y. Cao, L. Zhang, X. Yan, X. Zhang, S. Miao, Y. Tao, H. Li, C. Zheng, W. Huang and R. Chen, *Sci. Adv.*, 2022, **8**, eabk2925.
4 Y. Ren, W. Dai, S. Guo, L. Dong, S. Huang, J. Shi, B. Tong, N. Hao, L. Li, Z. Cai and Y. Dong, *J. Am. Chem. Soc.*, 2022, **144**, 1361.
5 A. Huang, J. Huang, H.-Y. Luo, Z.-W. Luo, P. Wang, P. Wang, Y. Guan and H.-L. Xie, *J. Mater. Chem. C*, 2023, **11**, 4104.
6 H. Su, K. Hu, W. Huang, T. Wang, X. Zhang, B. Chen, H. Miao, X. Zhang and G. Zhang, *Angew. Chem., Int. Ed.*, 2023, **62**, e202218712.
7 Y. Zhang, W. Zhang, J. Xia, C. Xiong, G. Li, X. Li, P. Sun, J. Shi, B. Tong, Z. Cai and Y. Dong, *Angew. Chem., Int. Ed.*, 2023, **62**, e202314273.
8 Z. Deng, J. Zhang, J. Zhou, W. Shen, Y. Zuo, J. Wang, S. Yang, J. Liu, Y. Chen, C.-C. Chen, G. Jia, P. Alam, J. W. Y. Lam and B. Z. Tang, *Adv. Mater.*, 2024, **36**, 2311384.
9 L. Zhou, J. Song, Z. He, Y. Liu, P. Jiang, T. Li and X. Ma, *Angew. Chem., Int. Ed.*, 2024, **63**, e202403773.
10 S. Hirata and M. Vacha, *J. Phys. Chem. Lett.*, 2016, **7**, 1539.
11 H. Li, H. Li, W. Wang, Y. Tao, S. Wang, Q. Yang, Y. Jiang, C. Zheng, W. Huang and R. Chen, *Angew. Chem., Int. Ed.*, 2020, **59**, 4756.
12 X. Wang, S. Ma, B. Zhao and J. Deng, *Adv. Funct. Mater.*, 2023, **33**, 2214364.
13 B. Chen, W. Huang and G. Zhang, *Nat. Commun.*, 2023, **14**, 1514.
14 L. Cheng, K. Liu, Y. Duan, H. Duan, Y. Li, M. Gao and L. Cao, *CCS Chem.*, 2020, **3**, 2749.

15 L. Wang, A. Hao and P. Xing, *ACS Appl. Mater. Interfaces*, 2022, **14**, 44902.

16 M. Zeng, W. Wang, S. Zhang, Z. Gao, Y. Yan, Y. Liu, Y. Qi, X. Yan, W. Zhao, X. Zhang, N. Guo, H. Li, H. Li, G. Xie, Y. Tao, R. Chen and W. Huang, *Nat. Commun.*, 2024, **15**, 3053.

17 G. Lu, Z.-G. Wu, R. Wu, X. Cao, L. Zhou, Y.-X. Zheng and C. Yang, *Adv. Funct. Mater.*, 2021, **31**, 2102898.

18 S. Sun, X. Li, C. Xu, Y. Li, Y. Wu, B. L. Feringa, H. Tian and X. Ma, *Natl. Sci. Rev.*, 2023, **10**, nwad072.

19 H. Yan, Y. He, D. Wang, T. Han and B. Z. Tang, *Aggregate*, 2023, **4**, e331.

20 L. Liu, J. Chen, T. Yu, R. Hu, G. Yang, Y. Zeng and Y. Li, *Chin. Chem. Lett.*, 2023, **34**, 107649.

21 J. Liu, Z.-P. Song, J. Wei, J.-J. Wu, M.-Z. Wang, J.-G. Li, Y. Ma, B.-X. Li, Y.-Q. Lu and Q. Zhao, *Adv. Mater.*, 2024, **36**, 2306834.

22 L. Gu, W. Ye, X. Liang, A. Lv, H. Ma, M. Singh, W. Jia, Z. Shen, Y. Guo, Y. Gao, H. Chen, D. Wang, Y. Wu, J. Liu, H. Wang, Y.-X. Zheng, Z. An, W. Huang and Y. Zhao, *J. Am. Chem. Soc.*, 2021, **143**, 18527.

23 K. Velmurugan, A. Murtaza, A. Saeed, J. Li, K. Wang, M. Zuo, Q. Liu and X.-Y. Hu, *CCS Chem.*, 2022, **4**, 3426.

24 L. Zhang, Y. Jin, Y. Wang, W. Li, Z. Guo, J. Zhang, L. Yuan, C. Zheng, Y. Zheng and R. Chen, *ACS Appl. Mater. Interfaces*, 2023, **15**, 49623.

25 J. Li, Y. Xie, Z. Feng, C. Zhang, H. Zhang, X. Chen and G. Zou, *J. Mater. Chem. C*, 2022, **10**, 16556.

26 C. He and Y. Li, *Chin. Chem. Lett.*, 2023, **34**, 108077.

27 Z. Xu, Y. He, H. Shi and Z. An, *SmartMat*, 2023, **4**, e1139.

28 X. Luo, J. Li, J. Zhao, L. Gu, X. Qian and Y. Yang, *Chin. Chem. Lett.*, 2019, **30**, 839.

29 W. Dai, Y. Zhang, X. Wu, S. Guo, J. Ma, J. Shi, B. Tong, Z. Cai, H. Xie and Y. Dong, *CCS Chem.*, 2021, **4**, 2550.

30 M. Xu, X. Li, S. Liu, L. Zhang and W. Xie, *Mater. Chem. Front.*, 2023, **7**, 4744.

31 F. Lin, J. Chen, Y. Miao, X. Long, W. Wang, W. Hu, H. Wang, H. Huang, G. Liang and Z. Chi, *J. Mater. Chem. C*, 2024, **12**, 3924.

32 T. Zhang, X. Ma and H. Tian, *Chem. Sci.*, 2020, **11**, 482.

33 F. Liao, J. Du, X. Nie, Z. Wu, H. Su, W. Huang, T. Wang, B. Chen, J. Jiang, X. Zhang and G. Zhang, *Dyes Pigm.*, 2021, **193**, 109505.

34 B. Wang, Z. Sun, J. Yu, G. I. N. Waterhouse, S. Lu and B. Yang, *SmartMat*, 2022, **3**, 337.

35 J. Bai, G. Dai, H. Jin, J. Ma, Z. Li, Y. Guan, M. Chen, Z. Ma and Z. Ma, *J. Mater. Chem. C*, 2023, **11**, 16325.

36 C. Shen, T. Jiang, Q. Lou, W. Zhao, C. Lv, G. Zheng, H. Liu, P. Li, L. Dai, K. Liu, J. Zang, F. Wang, L. Dong, S. Qu, Z. Cheng and C. Shan, *SmartMat*, 2022, **3**, 269.

37 F. Xiao, H. Gao, Y. Lei, W. Dai, M. Liu, X. Zheng, Z. Cai, X. Huang, H. Wu and D. Ding, *Nat. Commun.*, 2022, **13**, 186.

38 H. Sun and L. Zhu, *Aggregate*, 2023, **4**, e253.

39 Y. Zhao, J. Yang, C. Liang, Z. Wang, Y. Zhang, G. Li, J. Qu, X. Wang, Y. Zhang, P. Sun, J. Shi, B. Tong, H.-Y. Xie, Z. Cai and Y. Dong, *Angew. Chem., Int. Ed.*, 2023, **62**, e202317431.

40 T. Ono, K. Kimura, M. Ihara, Y. Yamanaka, M. Sasaki, H. Mori and Y. Hisaeda, *Chem. – Eur. J.*, 2021, **27**, 9535.

41 N. Feng, Z. Wang, D. Sun, P. Sun, X. Xin, X. Cheng and H. Li, *Adv. Opt. Mater.*, 2022, **10**, 2102319.

42 T. Zhu, T. Yang, Q. Zhang and W. Z. Yuan, *Nat. Commun.*, 2022, **13**, 2658.

43 S. Kuila, A. Ghorai, P. K. Samanta, R. B. K. Siram, S. K. Pati, K. S. Narayan and S. J. George, *Chem. – Eur. J.*, 2019, **25**, 16007.

44 X. Liang, T.-T. Liu, Z.-P. Yan, Y. Zhou, J. Su, X.-F. Luo, Z.-G. Wu, Y. Wang, Y.-X. Zheng and J.-L. Zuo, *Angew. Chem., Int. Ed.*, 2019, **58**, 17220.

45 Y. Sun, Z. Lei and H. Ma, *J. Mater. Chem. C*, 2022, **10**, 14834.

46 Z.-P. Yan, X.-F. Luo, W.-Q. Liu, Z.-G. Wu, X. Liang, K. Liao, Y. Wang, Y.-X. Zheng, L. Zhou, J.-L. Zuo, Y. Pan and H. Zhang, *Chem. – Eur. J.*, 2019, **25**, 5672.

47 C. Zhang, S. Li, X.-Y. Dong and S.-Q. Zang, *Aggregate*, 2021, **2**, e48.

48 J. Yang, Y. Zhang, X. Wu, W. Dai, D. Chen, J. Shi, B. Tong, Q. Peng, H. Xie, Z. Cai, Y. Dong and X. Zhang, *Nat. Commun.*, 2021, **12**, 4883.

49 W. Yang, N. Li, J. Miao, L. Zhan, S. Gong, Z. Huang and C. Yang, *CCS Chem.*, 2022, **4**, 3463.

50 Y. Zhang, S. Yu, B. Han, Y. Zhou, X. Zhang, X. Gao and Z. Tang, *Matter*, 2022, **5**, 837.

51 X. Wang, B. Zhao and J. Deng, *Adv. Mater.*, 2023, **35**, 2304405.

52 Y. Hu, Z. Huang, I. Willner and X. Ma, *CCS Chem.*, 2023, **6**, 518.

53 Y. Lei, W. Dai, J. Guan, S. Guo, F. Ren, Y. Zhou, J. Shi, B. Tong, Z. Cai, J. Zheng and Y. Dong, *Angew. Chem., Int. Ed.*, 2020, **59**, 16054.

54 B. Chen, W. Huang, X. Nie, F. Liao, H. Miao, X. Zhang and G. Zhang, *Angew. Chem., Int. Ed.*, 2021, **60**, 16970.

55 W. Dai, X. Niu, X. Wu, Y. Ren, Y. Zhang, G. Li, H. Su, Y. Lei, J. Xiao, J. Shi, B. Tong, Z. Cai and Y. Dong, *Angew. Chem., Int. Ed.*, 2022, **61**, e202200236.

56 W. Dai, G. Li, Y. Zhang, Y. Ren, Y. Lei, J. Shi, B. Tong, Z. Cai and Y. Dong, *Adv. Funct. Mater.*, 2023, **33**, 2210102.

57 Y. Lei, W. Dai, G. Li, Y. Zhang, X. Huang, Z. Cai and Y. Dong, *J. Phys. Chem. Lett.*, 2023, **14**, 1794.

58 G. Zhang, H. Ning, H. Chen, Q. Jiang, J. Jiang, P. Han, L. Dang, M. Xu, M. Shao, F. He and Q. Wu, *Joule*, 2021, **5**, 931.

59 H. Ning, G. Zhang, H. Chen, Z. Wang, S. Ni, F. Lu, F. Liu, L. Dang, J. Liu, F. He and Q. Wu, *Chem. Mater.*, 2021, **33**, 1976.

60 W. Dai, T. Bianconi, E. Ferraguzzi, X. Wu, Y. Lei, J. Shi, B. Tong, B. Carlotti, Z. Cai and Y. Dong, *ACS Mater. Lett.*, 2021, **3**, 1767.

61 X. Liu, W. Dai, J. Qian, Y. Lei, M. Liu, Z. Cai, X. Huang, H. Wu and Y. Dong, *J. Mater. Chem. C*, 2021, **9**, 3391.

This journal is © The Royal Society of Chemistry 2024

J. Mater. Chem. C, 2024, **12**, 9578–9585 | **9585**